Macromolecules

ARTICLE

pubs.acs.org/Macromolecules

Dual Stimuli-Responsive Poly(2-hydroxyethyl methacrylate-*co*-methacrylic acid) Microgels Based on Photo-Cleavable Cross-Linkers: pH-Dependent Swelling and Light-Induced Degradation

Daniel Klinger and Katharina Landfester*

Max Planck Institute for Polymer Research, Ackermannweg 10, 55128 Mainz, Germany

Supporting Information

ABSTRACT: Dual stimuli-responsive p(HEMA-*co*-MAA) microgels were prepared in a facile way by inverse miniemulsion copolymerization of 2-hydroxyethyl methacrylate (HEMA) with methacrylic acid (MAA) and two kinds of newly synthesized photodegradable cross-linkers. The pH-dependent swelling behavior induced by the protonation/deprotonation of the methacrylic acid groups in the network-forming polymer was investigated by means of the particle volume change as determined by DLS measurements. Photolytic degradation experiments were conducted by irradiation with UV light which led to particle disintegration caused by cleavage of the photolabile cross-linking points. The degradation behavior of the microgels was investigated with respect to degradation rates and changes in the degree of swelling. Those parameters were found to depend on the pH value of the solvent, the light intensities, and the irradiation wavelengths applied. For similar conditions, the degradation profile was demonstrated to strongly depend not only on the molecular structure of the cross-linking molecule but also on the molecular weight of the network-forming copolymers. The particular combination of the stimuli described is designed as a new strategy to two different swelling/degradation profiles. This dual stimuli-responsiveness was shown to enable the efficient loading and subsequent release of myoglobin as a model protein. Here a slow diffusion controlled release (induced by changes of the pH) was combined with a fast degradation controlled (induced by irradiation) on-demand release. This novel two-step release profile is proposed to bear great potential for delivery applications.

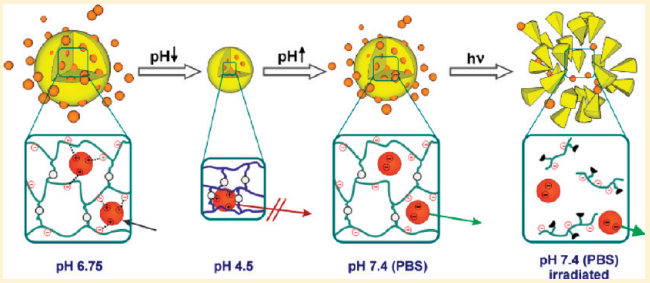

INTRODUCTION

Since the discovery of microgels as a unique class of polymeric nanoscale materials, this research area has gained increasing attention. In general, the exceptional properties of microgels stem from the combination of their colloidal nature with their internal network structure.[1] These 3-dimensional networks in the nanoscale represent highly functional materials exhibiting bespoken properties for a tremendous variety of applications such as sensors,[2] optics,[3,4] colloidal crystals,[4,5] and release applications in materials science[6−8] and biomedical fields.[9,10]

Regarding the development of microgels for release applications in general, one of the main tasks is to combine an efficient loading process with a well-defined release profile.[11] Here, it is of high interest to prevent leakage of the embedded functional compound until the targeted site or time point is reached. One interesting approach concept to realize this aim is based on the ability to control the diffusion of compounds in the network.[12,13] Since the latter is characterized by parameters such as the mesh size, the polymer volume fraction or the interaction of embedded functional compounds with the network, the ability to control these factors by the application of external triggers represents the underlying concept to stimuli-responsive microgels.[14,15]

One interesting class of stimuli-responsive microgels for release applications is based on changing the physicochemical properties of the network-forming polymers upon application of an external trigger. This concept is mainly realized by either temperature-[16,17] or pH-sensitive gel particles[14,18−20] and can be applied for controlling the diffusion of a payload by several mechanisms: (i) triggered swelling and deswelling[13,21,22] allows the adjustment of mesh sizes relative to the hydrodynamic radii of the functional substances (e.g., proteins, enzymes, catalytic metal nanoparticles);[23] (ii) ionization/deionization of a network-forming polyelectrolyte allows the adjustment of electrostatic interactions of e.g. small molecules with the polymeric matrix[24,25] and (iii) embedding compounds into initially collapsed networks[26]—thus excluding water from the gel interior—prevents diffusion prior to a triggered swelling-induced release.

An alternative approach to achiev e controlled release out of gels is based on the use of cleavable cross-linking points allowing the complete decomposition of the network architecture by using external stimuli. In the context of such degradation

Received: July 25, 2011
Revised: November 4, 2011
Published: November 28, 2011

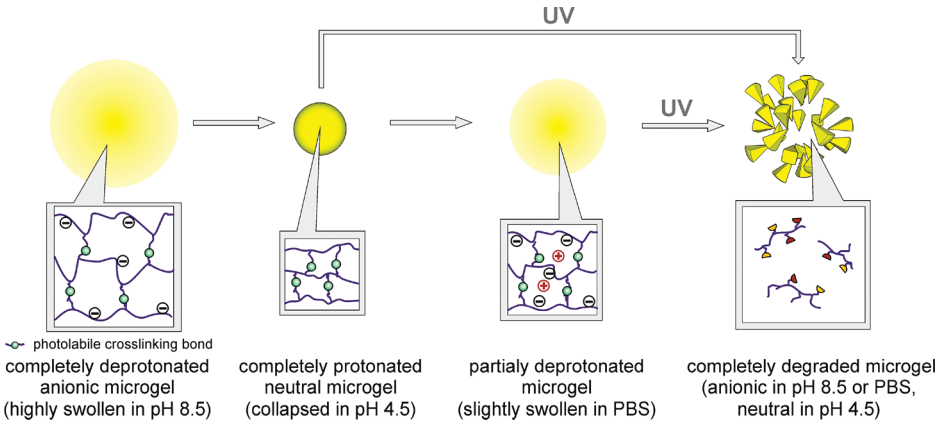

Figure 1. Schematic representation of the double stimuli-responsive character of the photodegradable p(HEMA-*co*-MAA) microgels.

controlled delivery systems, e.g., enzyme-sensitive microgels containing dextran-based cross-linkers,[27,28] reducing agent sensitive cross-linkers based on disulfide bonds,[29] or acid-degradable microgels synthesized with cross-linkers based on tertiary esters[30] or acetals,[31,32] have been investigated for delivery systems in organic and aqueous media. Here, relatively large functional compounds—such as, e.g., DNA[31] or proteins[33]—are primarily entrapped in a network due to initial mesh sizes smaller than the hydrodynamic diameters of the respective compounds to be delivered. Upon the degradation of cross-linking points, the cross-linking density decreases which results in increased mesh sizes. Thus, the release of functional compounds is enabled.

Regarding particulate delivery systems solely based on pH-sensitive materials, either degradation or diffusion controlled release occurs as a response to the H^+ concentration of the local environment, thus rendering those particles "smart". Such concepts are investigated for drug delivery applications by exploiting the acidic pH of malignant tissue and lysosomes.[23,34] Nevertheless, these systems require the addition of protons or the localization in acidic milieus.

In comparison, inducing the release of a payload by applying an external trigger without a change in the chemical composition of the surrounding media bears the advantage of an on-demand delivery. Concerning this point, light represents an outstanding position as it can be applied in a very precise manner by selecting suitable wavelengths, polarization directions and intensities in a noncontact approach. In addition, light offers the possibility to change the polymer properties in very confined spaces and time scales. Exploiting these advantages for triggered release applications can in general be realized by the utilization of a broad variety of chromophores. Among those, *o*-nitrobenzyl moieties are very attractive due to the fast and quantitative reaction of the chromophore upon irradiation with UV light.[35,36] The good photolytic properties in various solvents and even the solid[37] or macromolecular[38,39] state render those moieties highly interesting for a broad variety of applications.[40,41] In particular, the tunable[36] enhanced absorption for wavelengths of $\lambda > 300$ nm enables photoreactions to be carried out in a controlled manner and under mild conditions suitable for biological applications.[42,43] Recent investigations based on light-sensitive materials for release applications include photoswitchable block copolymer micelles for the delivery of hydrophobic compounds[44−47] as well as photoresponsive nanocarriers based on capped dendrimers[48] or hyperbranched polyglycerol nanocapsules.[49] Additionally, we recently reported on the formation of light-sensitive PMMA microgels containing photodegradable cross-linking points based on *o*-nitrobenzyl moieties.[50] Since these materials exhibited well pronounced light-triggered swelling and degradation profiles in organic solvents, it is highly interesting to transfer this concept to aqueous media by the incorporation of such cross-linking molecules into hydrogel nanoparticles and to investigate the potential of these materials for loading and release applications.

On the basis of these considerations, the aim of this work is the preparation of dual stimuli-responsive microgels to exhibit a pH-dependent volume phase transition due to ionizable methacrylic acid (MAA) groups in poly(2-hydroxyethyl methacrylate) (PHEMA) as network-forming polymer and the ability to complete particle disintegration upon irradiation due to light-cleavable cross-linking points. The particular combination of the mentioned stimuli is designed to exhibit two different degradation profiles as shown in Figure 1. In both cases, particles are proposed to be highly swollen for pH values higher than the pK_a of the microgels, whereas decreasing the pH leads to a deswelling of the networks.[24,25] The disintegration of the collapsed particles by direct irradiation represents a one-step degradation profile. In contrast, by transferring the collapsed particles to phosphate buffered saline (PBS), slightly swollen particles are obtained, which can subsequently be degraded by the application of UV light, therefore characterizing a two-step swelling/degradation profile.

EXPERIMENTAL SECTION

Materials. All chemicals were purchased from Sigma-Aldrich and used without further purification unless otherwise stated. 2-Hydroxyethyl methacrylate (HEMA) and methacrylic acid (MAA) were freshly distilled under reduced pressure prior to use.

Instrumentation. ^{1}H (300 MHz) and ^{13}C NMR (75 MHz) spectra were measured using a Bruker spectrometer. Particle size distributions were determined by dynamic light scattering (DLS) using a NICOMP Zetasizer measuring at a fixed scattering angle of 90°. The measurements were carried out at 25 °C on diluted dispersions in the respective solvents. A Perkin-Elmer Lambda 25 UV−vis spectrometer was used to measure UV−vis spectra. Irradiations were either carried out by using a 365 nm emitting UV-LED with a maximum power of 150 W or an OSRAM HBO 100 W/2 mercury short arc lamp combined with a UG-11 and a W-320 filter resulting in an output of wavelengths of $\lambda = 315-390$ nm. HPLC measurements were conducted using an Agilent quarternary gradient pump (series 1100) combined with an Agilent photodiode array detector (DAD series 1200). A Gemini 1530 (Carl Zeiss AG, Oberkochem,

Scheme 1. Synthesis of Photolabile Cross-Linkers: Reagents and Conditions[a]

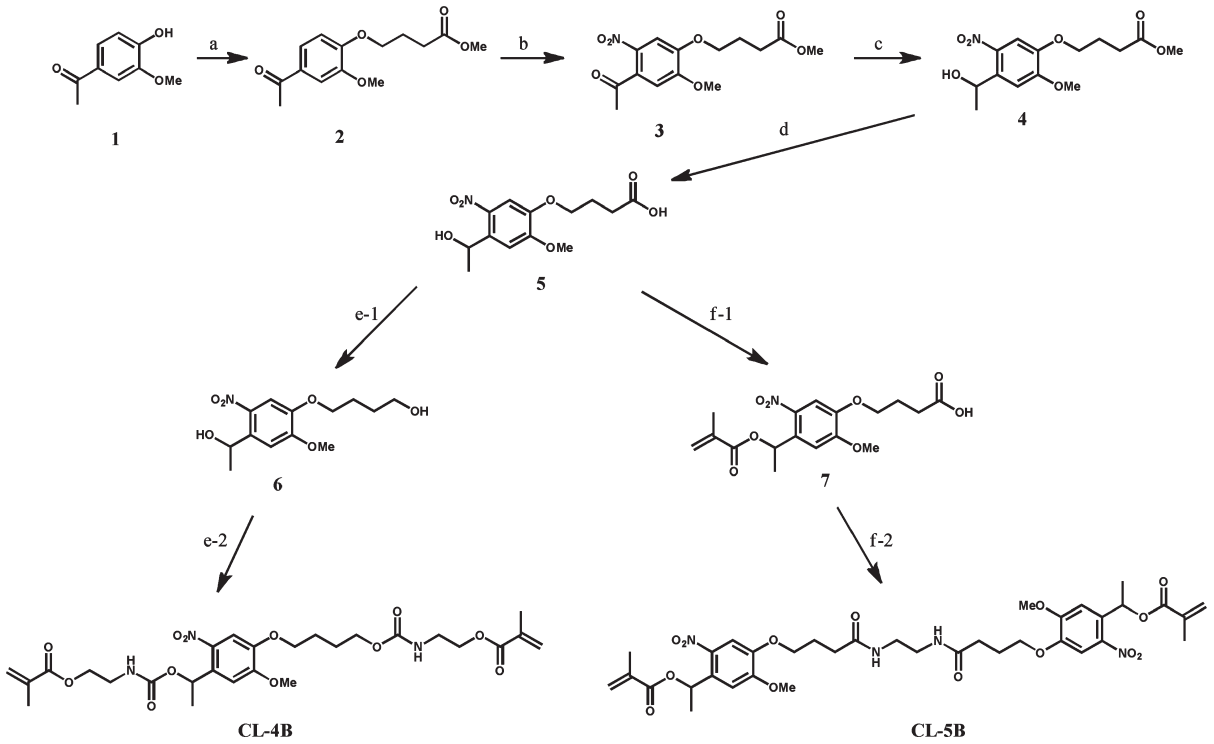

[a] Key: (a) methyl 4-bromobutyrate, K_2CO_3/DMF (anhyd.), 25 °C, 16 h, quant.; (b) acetic anhydride/nitric acid (1:2, v/v), 0 °C, 3 h, 53%; (c,d) $NaBH_4$/MeOH/THF, 25 °C, 16 h, NaOH, 25 °C, 7 h, 89%; (e-1) BH_3*THF/THF, 0°C, 1 h then 40 °C, 18 h, 86%; (e-2) 2-isocyanatoethyl methacrylate, DBTDL (cat.)/THF, 65 °C, 48 h, 63%; (f-1) methacryloyl chloride, NEt_3/DCM, 0 to 25 °C, 15 h, 42%; (f-2) ethylenediamine, DCC, DMAP (cat.)/DCM, 0 to 25 °C, 15 h, 53%.

Germany) with an InLens detector was used to take scanning electron micrographs (SEM). The samples were prepared by drop-casting of diluted dispersions on a silicon wafer. UV−vis measurements for the loading and release experiments were performed on a Tecan plate reader.

Synthesis of Photo-Degradable Cross-Linkers. On the basis of the photolabile molecules of either 4-(4-(1-hydroxyethyl)-2-methoxy-5-nitrophenoxy)butan-1-ol (HEMNPB) or 4-(4-(1-hydroxyethyl)-2-methoxy-5-nitrophenoxy)butanoic acid (HEMNPBA), two different cross-linkers were synthesized. The synthetic concept is presented in Scheme 1.

4-(4-(1-Hydroxyethyl)-2-methoxy-5-nitrophenoxy)butanoic acid (HEMNPBA) (5). As described in a previous publication,[50] the product was prepared based on the synthetic protocols by Holmes.[36,51] Briefly, acetovanillone was reacted with methyl 4-bromobutyrate in the presence of potassium carbonate to form the corresponding keto ester. After removing the inorganic salts by extraction with ethyl actetate, subsequent nitration of the crude product was achieved by the reaction with acetic anhydride and nitric acid (1:2 v/v). In the next step, the reduction of the keto group with excess borohydride was conducted and directly followed by inducing the ester cleavage by the addition of NaOH in water. Purification by recrystallization from ethyl acetatet/hexane afforded HEMNPBA (**5**) in 89% yield as a pale yellow solid.

^{1}H NMR ($CDCl_3$): δ = 7.41 (s, 1H), 7.24 (s, 1H), 5.37 (q, J = 6.2 Hz, 1H), 3.97 (t, J = 6.4 Hz, 2H), 3.82 (s, 3H), 2.37 (t, J = 7.2 Hz, 2H), 2.00 (p, J = 6.8 Hz, 3H), 1.35 (d, J = 6.3 Hz, 1H). ^{13}C NMR ($CDCl_3$): δ = 174.92, 154.05, 146.56, 139.12, 138.33, 108.97, 108.89, 68.24, 64.95, 56.23, 30.18, 24.84, 24.18. MS (FD): m/z 299.2 (M^+).

4-(4-(1-Hydroxyethyl)-2-methoxy-5-nitrophenoxy)butan-1-ol (HEMNPB) (6). The photolabile molecule HEMNPB was obtained by reduction of the carboxy group with 2.5 equiv of $BH_3 \cdot$THF in THF for 18 h at 40 °C. The destruction of excess borane by adding water was followed by extracting the mixture with ethyl acetate. The dried organic layers were recrystallized from chloroform yielding pure HEMNPB (**6**) in 86% yield.

^{1}H NMR ($CDCl_3$): δ = 7.55 (s, 1H), 7.29 (s, 1H), 5.55 (q, 1H, J = 6.3 Hz), 4.10 (t, 2H, J = 6.1 Hz), 3.97 (s, 3H), 3.73 (t, 2H, J = 6.2 Hz), 1.98 (m, 2H), 1.77 (m, 2H), 1.55 (d, 3H, J = 6.3 Hz). ^{13}C NMR ($CDCl_3$): δ = 153.67, 146.38, 138.87, 137.94, 108.62, 108.30, 68.91, 64.65, 61.40, 55.96, 28.89, 25.23, 24.60. MS (FD): m/z 285.0 (M^+).

2-((1-(4-(4-(2-(Methacryloyloxy)ethylcarbamoyloxy)butoxy)-5-methoxy-2-nitrophenyl)ethoxy)carbonylamino)-ethyl methacrylate (CL-A). Synthesis was performed according to the literature[50] by the reaction of 2-isocyanatoethyl methacrylate with HEMNPB (**6**) and dibutyltin dilaurate in anhydrous THF. Purification by column chromatography over silica using $CHCl_3$/MeOH (10:1) as eluent yielded CL-A as slightly yellow colored oil; yield 63%.

^{1}H NMR ($CDCl_3$): δ = 7.56 (s, 1H), 6.98 (s, 1H), 6.37 (q, 1H, J = 6.3 Hz), 6.10 (d, 2H, J = 7.7 Hz), 5.59 (m, 2H), 5.06 (s, 1H), 4.96 (t, 1H), 4.13 (m, 8H), 3.93 (s, 1H), 3.48 (m, 4H), 1.93 (d, 6H, J = 4.6 Hz), 1.81 (m, 4H), 1.81 (m, 1H),1.59 (d, 3H, J = 6.3 Hz). ^{13}C NMR ($CDCl_3$): δ = 167.29, 156.47, 155.20, 153.97, 147.20, 139.69, 135.96, 133.81, 126.05, 108.92, 69.10, 68.85, 64.48, 63.70, 63.65, 56.30, 40.18, 25.62, 25.46, 22.17, 18.27. MS (FD): m/z 595.5 (M^+).

4-(4-(1-(Methacryloyloxy)ethyl)-2-methoxy-5-nitrophenoxy)butanoic acid (7). To an ice-cooled suspension of **5** (1.750 g, 5.85 mmol) and triethylamine (1.775 g, 17.54 mmol) in 70 mL of anhydrous DCM, methacryloyl chloride (1.746 g, 14.62 mmol) was added dropwise at 0 °C under argon atmosphere. The reaction mixture was allowed to warm to room temperature while stirring

overnight and the resulting solution was washed with Na_2CO_3 (5%), HCl (1%), and water. The organic solvent was evaporated, the residue was dissolved in acetone/water and stirred overnight, insoluble components were removed by filtration and the mixture was extracted with DCM. After washing the resulting solution with HCl (1%) and water, the organic phase was dried over $MgSO_4$ and the solvent was removed. Purification by column chromatography over silica using MeOH/$CHCl_3$ (1:5 v/v) as eluent yielded pure **7** in 43% yield.

^{1}H NMR ($CDCl_3$): δ = 7.59 (s, 1H), 7.02 (s, 1H), 6.52 (q, 1H), 6.17 (s, 1H), 5.61 (s, 1H), 4.12 (t, 2H), 3.92 (s, 3H), 2.61 (t, 2H), 2.19 (qnt, 2H), 1.95 (s, 3H), 1.66 (d, 3H). ^{13}C NMR ($CDCl_3$): δ = 178.21, 166.08, 154.01, 147.12, 139.76, 136.35, 133.58, 125.73, 109.10, 108.11, 68.76, 68.04, 56.20, 30.21, 23.99, 22.04, 18.32.

1,1′-(4,4′-(4,4′-(Ethane-1,2-diylbis(azanediyl))bis(4-oxobutane-4,1-diyl))bis(oxy)bis(5-methoxy-2-nitro-4,1-phenylene))-bis(ethane-1,1-diyl)bis(2-methyl acrylate) (CL-B). A solution of **7** (0.847 g, 2.30 mmol), DMAP (0.054 g, 0.44 mmol) and ethylene diamine (0.065 g, 1.10 mmol) in 40 mL of anhydrous DCM was cooled to 0 °C and stirred at this temperature for 30 min. DCC (0.520 g, 2.52 mmol) was dissolved in 10 mL of anhydrous DCM and added to the reaction mixture which was allowed to warm to room temperature while stirring overnight. Filtration to remove the produced urea was followed by washing the organic solution with saturated NH_4Cl, saturated Na_2CO_3, and brine. The organic phase was dried over $MgSO_4$ and the solvent was evaporated under reduced pressure. The resulting residue was purified by column chromatography using silica and MeOH/$CHCl_3$ as eluent yielding pure CL-B as a pale yellow solid (0.422 g, 0.56 mmol). Yield 51%.

^{1}H NMR ($CDCl_3$): δ = 7.58 (s, 2H), 7.01 (s, 2H), 6.50 (q, 2H), 6.46 (s, 2H), 6.17 (s, 2H), 5.61 (s, 2H), 4.09 (t, 4H), 3.92 (s, 6H), 3.38 (dd, 4H), 2.40 (t, 4H), 2.16 (qnt, 4H), 1.95 (s, 6H), 1.65 (d, 6H). ^{13}C NMR ($CDCl_3$): δ = 173.44, 166.23, 154.02, 147.23, 139.96, 136.46, 133.68, 125.89, 109.21, 108.24, 68.87, 68.70, 56.39, 40.38, 32.90, 24.88, 22.14, 18.43. MS (FD): m/z 759.6 ($M + 1^+$), 1518.1 ($2M^+$).

Photo-Degradation Studies of Cross-linkers in Solution via ^{1}H NMR and Mass Spectroscopy. Cross-linkers were dissolved in THF with a concentration of 3.0×10^{-3} mol/L. Irradiations were performed in a quartz cuvette for 10 h using a mercury short arc lamp combined with the described filters and an intensity of I = 17 mW/cm^2 for the wavelengths of λ = 315−390 nm. The reaction mixture was divided into two fractions and both were evaporated to dryness under reduced pressure. One fraction was investigated by ^{1}H NMR spectroscopy, the other fraction was investigated by field desorption mass spectrometry.

Photo-Degradation Studies by UV−Vis Measurements. A quartz cuvette containing a solution ($c = 4.5 \times 10^{-4}$ mol/L) of the respective cross-linker in THF was placed under a UV lamp (λ = 315−390 nm, I = 17 mW/cm^2) and the samples were irradiated for fixed time intervals. UV−vis measurements were performed subsequently.

Kinetic HPLC Measurements. Cross-linker solutions in THF were prepared and irradiated analogously to those used for the ^{1}H NMR spectroscopic measurements. Samples were taken at fixed time intervals and directly measured by HPLC using a solvent gradient of THF/water from 40/60 to 30/70. Photolytic conversion of the cross-linkers was determined by the decrease of the peak area of the starting compound.

Preparation of Cross-Linked Photo-Degradable p(HEMA-*co*-MAA) Gel Particles by Inverse Miniemulsion Polymerization. Cross-linked p(HEMA-*co*-MAA) microgels (MG) were synthesized by free radical copolymerization in inverse miniemulsion. Microgels MG-10 and MG-1A were prepared by first mixing HEMA (1.275 g, 9.8 mmol), MAA (0.225 g, 2.6 mmol), water (70 mg, 3.9 mmol), and 2.5 mol % of the respective cross-linker. In case of the microgels MG-20, MG-2A, and MG-2B, additional DMSO (0.375 g) as solvent was added. Afterward, the mixture was added to the continuous phase consisting of a solution of the amphiphilic block copolymer P(E/B)-*b*-PEG (75 mg) as nonionic surfactant in 12.5 g of cyclohexane. The miniemulsion was formed by first stirring the mixture at 1750 rpm for 1.5 h and then homogenizing the obtained pre-emulsion by ultrasonication for 2 min at 90% intensity (Branson sonifier W450 Digital, 0.5 in. tip) at 0 °C. 2,2′-Azobis(2-methyl-butyronitrile) (V-59) (50 mg, 0.3 mmol) as thermal initiator was added and polymerizations were then carried out overnight in an oil bath set at 70 °C. The used amounts of cross-linkers and DMSO for the different reactions are summarized in Table 1.

Table 1. Synthetic Details for the Miniemulsion Polymerizations of p(HEMA-*co*-MAA) Microgels

		cross-linker		
sample	DMSO (m/mg)	type	amount, m/mg	amount, mol %
MG-10	---	---	---	---
MG-1A	---	CL-A	185	2.5
MG-20	375	---	---	---
MG-2A	375	CL-A	185	2.5
MG-2B	375	CL-B	235	2.5

After the polymerization, coagulates were removed by filtration over kimwipe paper and the resulting dispersions were centrifuged at 10 000 rpm for 30 min to collect the particles. The supernatant was removed and replaced by cyclohexane. Redispersion was carried out using a vortex. In order to remove excess surfactant, the dispersions were further washed four times with cyclohexane, following the procedure described above. The purified dispersions of the MGs were examined with regard to the particle size distributions by means of dynamic light scattering (DLS) and scanning electron microscopy (SEM). Freeze-drying removed unreacted monomer and yielded the cross-linked p(HEMA-*co*-MAA) gel particles as white to slightly yellow colored powders. The freeze-dried particles were swollen overnight at 5% (w/v) in water adjusted to pH 12 at room temperature. Three additional washing steps by centrifugation at 17 500 rpm for 90 min at 15 °C and redispersion in deionized water were performed to remove the sol content which consisted of all the soluble polymers and non-cross-linked particles. The purified particles were freeze-dried and redispersed in the respective media by simple swelling at room temperature for 6 h at the desired concentration.

pH-Dependent Swelling Studies of Cross-Linked p(HEMA-*co*-MAA) Microgels. Particle size distributions were determined by DLS in water as described above. SEM analysis was conducted to determine the morphologies of the particles.

Photo-Degradation Studies of Cross-Linked Gel Particles in Water. Samples of 0.125% (w/v) MG in phosphate buffer saline (PBS) or water adjusted to the desired pH were placed in a quartz cuvette and irradiated with the respective UV light source. At predetermined times, samples were collected and turbidity measurements were conducted by using a NICOMP Zetasizer. The volume of the irradiated sample was retained by returning the withdrawn samples to the cuvette after every measurement. The turbidity was obtained by calculating the ratio of the scattering intensity at 90° of the irradiated samples relative to the one of the nonirradiated samples. Particle size distributions of the irradiated particle dispersions were obtained by DLS in the respective solvent. Furthermore, SEM images were taken to investigate the morphology of the irradiated particles.

Loading of p(HEMA-*co*-MAA) Microgels with Myoglobin and Subsequent Release Experiments. To 18 mL of a stock solution of myoglobin (c = 1 mg/mL) in water with a pH adjusted to pH 6.75 were added 2 mL of a dispersion of MG-2B p(HEMA-*co*-MAA) microgels in water (c = 1 mg/mL). The pH of the mixture was adjusted

Scheme 2. Photo-Reactions of the Cleavable Cross-Linkers: (a) CL-A and (b) CL-B

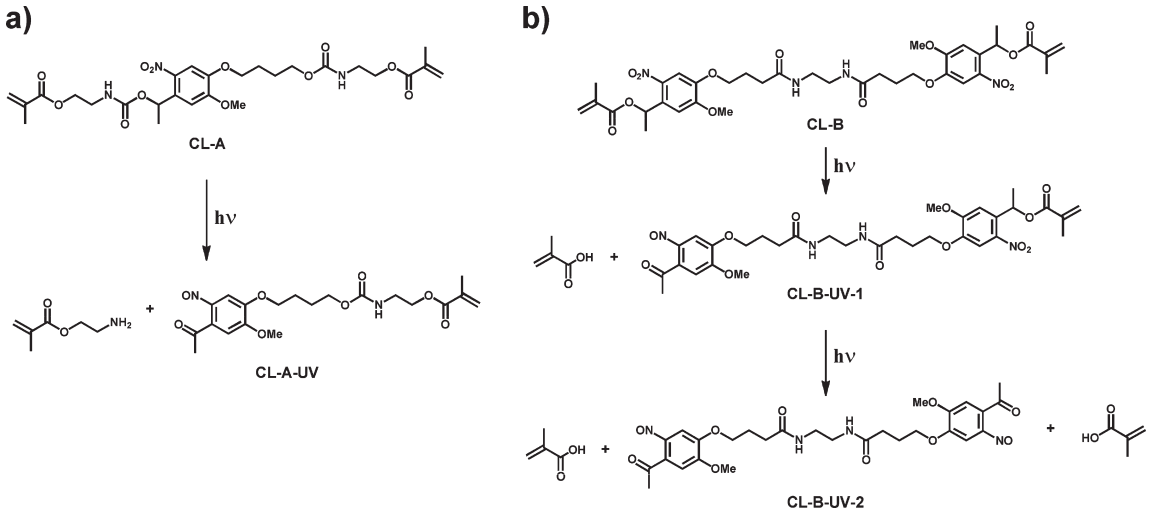

to pH 6.75 by the addition of diluted NaOH and HCl. After equilibration at room temperature overnight, the pH was adjusted to pH 4.5 by the addition of diluted HCl and the particles were collected by centrifugation (10 000 rpm; 30 min). The supernatant (20 mL) was examined by UV−vis spectroscopy. The pellet of the centrifugation was redispersed in 20 mL of water adjusted to pH 4.5 using a vortex. The loaded microgels were washed four more times following the described procedure and the supernatants of every washing step were investigated by UV−vis spectroscopy. Subsequently to the last centrifugation step, the microgels were redispersed in PBS with pH 7.4 (20 mL). A sample (2 mL) was taken and investigated by UV−vis spectroscopy. The dispersion of the loaded microgels in PBS was shaken at 37 °C and samples were taken after predetermined time intervals. The release of myoglobin into the surrounding medium was investigated by removing the microgels from each sample by centrifugation and comparing the UV−vis spectra of the supernatants to a calibration curve of myoglobin in PBS. Irradiation-induced release experiments were conducted by irradiating samples of 4 mL in a quartz cuvette under stirring for 90 min with UV light of the wavelengths of $\lambda = 315-390$ nm and an intensity of 17 mW/cm^2. The loading and release experiments were performed in duplicate and UV−vis measurements were conducted on 2 different dilutions of the samples. Every measurement was performed in triplicate using a Tecan plate reader. Reported values represent the average of all measurements and errors correspond to the respective standard deviation.

RESULTS AND DISCUSSION

The concept of novel light- and pH-sensitive p(HEMA-*co*-MAA) microgels was realized by combining two orthogonal approaches. The incorporation of MAA into the microgels resulted in a pH-dependent swelling behavior of the particles. Protonation/deprotonation of the carboxylic acid groups changed the physicochemical properties of the network-forming copolymers and therefore caused the collapse at low pH and the expansion at pH values higher than the apparent pK_a of the respective microgels. Light-sensitivity of the hydrogel particles was achieved by the utilization of two different photolabile cross-linking molecules. Irradiation of the microgels led to the degradation of the cross-linking points and therefore to the disintegration of the particle structure. This dual stimuli-responsive performance was designed to enable the independent pH-induced swelling/collapsing and the subsequent light-induced degradation of the microgels as shown in Figure 1.

This dual stimuli-responsive character was shown to enable the efficient loading and release of myoglobin as a model protein. A new two-step—pH-induced swelling followed by light-induced degradation—release profile was demonstrated.

Synthesis and Characterization of Photo-Labile Cross-Linkers. Two different types of photolabile cross-linkers were synthesized in order to investigate the influence of the molecular structure on the degradation behavior of the hydrogel particles. The synthetic pathway and the reaction conditions are shown in Scheme 1.

Both structures are based on 4-(4-(1-hydroxyethyl)-2-methoxy-5-nitrophenoxy)butanoic acid (HEMNPBA) which was synthesized accordingly to a previous publication.[50] Briefly, acetovanillone was reacted with methyl 4-bromobutyrate to the corresponding keto ester (**2**) under basic conditions. A subsequent nitration of the crude product was achieved by the reaction with acetic anhydride and nitric acid. In the next step, the reduction of the keto group of **3** with excess borohydride was conducted and directly followed by inducing the ester cleavage by the addition of NaOH in water yielding HEMNPBA (**5**). CL-A was synthesized by first reducing the acid group of **5** to the corresponding alcohol and then reacting **6** with 2 equiv of 2-isocyanatoethyl methacrylate in the presence of catalytic amounts of DBTDL to form the carbamate. In the case of CL-B, HEMNPBA (**5**) was reacted with an excess amount of methacryloyl chloride to form the *o*-nitrobenzyl ester of **7**. The symmetric cross-linker CL-B was then prepared by DCC coupling of 2 equiv of **7** with ethylene diamine.

Both cross-linkers are based on nitroveratryloxycarbonyl derivatives as the photoreactive moieties but vary in the way of the attachment of the polymerizable methacrylate units to the chromophore core. The *o*-nitrobenzyl group in general is characterized by its chemical stability and rapid cleavage upon exposure to UV light. The α-methyl group on the benzylic carbon of the *o*-nitrobenzyl core is known to increase the rate of photolysis significantly[52] and was therefore introduced into the molecules. Considering the abstraction of a benzylic proton by the photoactivated nitro group as the rate-limiting step in the photolysis of the *o*-nitrobenzyl group, the additional methyl group increases

the acidity of this proton. Furthermore, the introduction of alkoxy substituents in the *o*-nitrobenzylic core results in a considerably increased UV absorption for $\lambda > 315$ nm.[39]

Generally, photolysis of the cross-linkers only requires the irradiation wavelength to overlap with the absorption band of the photolabile chromophore. However, degradation of cross-linkers and the resulting p(HEMA-*co*-MAA) gel particles should be performed in a controlled manner under mild conditions. Thus, Norrish-type side reactions, which primarily take place for irradiations with wavelengths of $\lambda < 300$ nm,[53,54] should be avoided. In addition, to evade undesirable side effects in biological applications, irradiations with UV-A light of wavelengths $\lambda > 315$ nm is favored. UV−vis spectroscopy of the cross-linkers CL-A and CL-B showed in every case an absorption maximum at 300 nm and an additional absorption maximum at 342 nm (see Supporting Information). Thus, both cross-linkers exhibit a high absorption coefficient in the targeted photolysis wavelength region of $\lambda > 315$ nm.

Photolysis of the Cleavable Cross-Linkers in Solution. Although either type of cross-linker consists of one or two central *o*-nitrobenzylic group(s), the variation of the molecular attachment of the radically polymerizable methacrylate moieties onto the photolabile chromophore results in different photoproducts with specific functional groups. The respective photoreactions are depicted in Scheme 2.

The carbamate derivative of cross-linker CL-A degrades into an amine and a ketone (CL-A-UV), whereas irradiation of the ester of CL-B generates two carboxylic acid groups and a molecule containing two ketone moieties (CL-B-UV-2). Earlier investigations on the photolysis of CL-A revealed that upon longer irradiation times with UV light of the wavelengths of $\lambda > 300$ nm, dimeric azoxybenzene compounds are formed from the primary photoproducts (CL-A-UV) in THF solution. As shown for photodegradable PMMA microgels, the covalent attachment of those side products to the polymer backbone hinders complete particle degradation due to the formation of new cross-linking points in the respective gels.[50] Even though a dramatic increase in the degree of swelling for those particles could be detected for the mentioned irradiation conditions, complete microgel disintegration enhances the potential for delivery applications. Therefore, the symmetric molecular structure of CL-B was designed to generate only carboxylic acid groups on the polymer backbone by photolytic cleavage of the *o*-nitrobenzyl ester bonds. The separated middle part (CL−B-UV-2) of the cross-linking molecule contains both of the chromophore cores and is not connected to the gel-forming polymers any more (compare Scheme 2b). Thus, a possible formation of dimeric side products of the photoproduct is assumed to result in liberated molecules not hindering the particle degradation. In addition, the formed methacrylic acid groups for CL-B in the polymer backbone are supposed to enhance the swelling of the anionic gels whereas the amine groups generated upon photolysis of CL-A are—due to electrostatic interactions and dependent on the pH—able to form physical cross-links with the methacrylic acid groups in the p(HEMA-*co*-MAA) copolymer.

In comparison to the studies performed on CL-A,[50] the photodegradation behavior of the cross-linkers in equimolar THF solutions was first investigated by irradiation time-dependent UV−vis measurements. The respective spectra are shown in Figure S1 in the Supporting Information. Irradiation of either the CL-A or the CL-B cross-linker with UV light of the wavelengths $\lambda = 315-390$ nm resulted in every case in a red shift of the

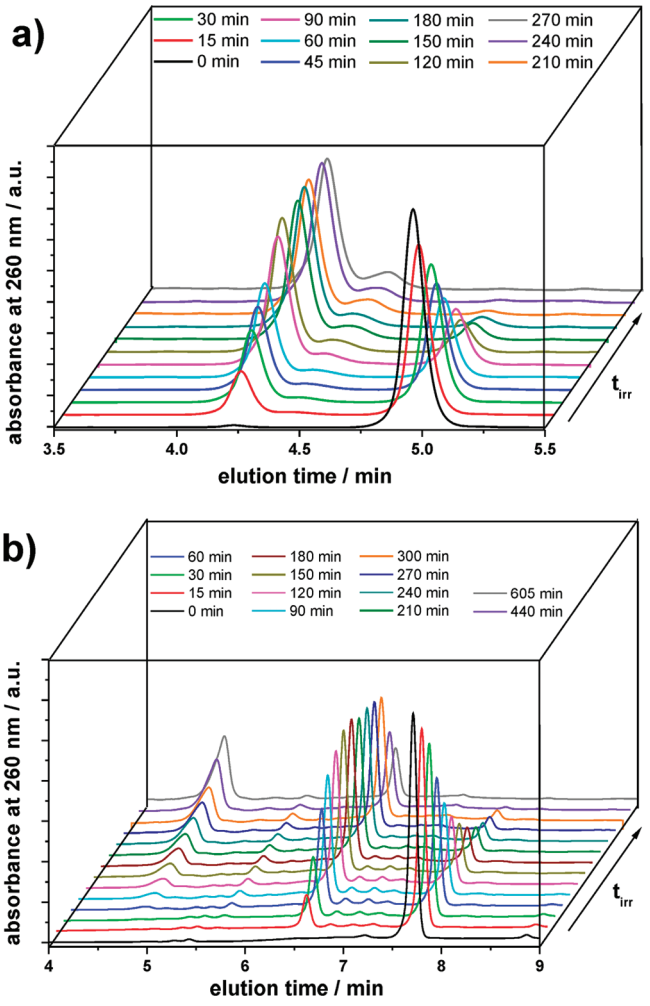

Figure 2. Investigations on the photolytic cross-linker degradation. Irradiation time-dependent HPLC measurements of (a) CL-A and (b) CL-B.

absorption maxima to $\lambda_{max} = 385$ nm. These light-induced changes of the absorption spectra point toward successful photoreactions. However, the formation of possible side products absorbing light in the same spectral region could not be excluded. In the case of CL-A, no further changes in the absorption spectra were detected after an irradiation time of 5 min indicating no further conversion of the photoreaction (see Supporting Information, Figure S1a). In comparison, more than 10 min of irradiation were necessary to complete the light-induced cleavage of the CL-B molecule (see Supporting Information, Figure S1b). Comparing the molecular structure of CL-A to CL-B, it becomes obvious that for the same molar concentration in THF, in the latter case two chromophores per molecule have to be cleaved. As a result, the required irradiation time is increased.

In order to perform a quantitative time-dependent degradation analysis of the cross-linkers, HPLC measurements were conducted to examine the composition of the reaction mixtures at various irradiation times (Figure 2, parts a and b). The kinetics of the photolysis of the photolabile molecules was therefore investigated by monitoring the rate of disappearance of the starting compounds during irradiation. Kinetic plots of $-\ln[CL]_t/[CL]_0$ versus time show all excellent linearity, indicating the

expected first order kinetic with respect to the chromophore concentration (see Figure 3). Figure 2 presents the time dependent HPLC elution curves of the photolysis of CL-A in comparison to those of CL-B. The kinetic plots for the calculation of the rate constants for both cross-linkers and obtained half-life times and rate constants are listed in Figure 3.

Both cross-linkers were found to degrade completely upon irradiation with UV light of wavelengths with λ = 315−390 nm. As shown before,[50] the elugram of cross-linker CL-A (Figure 2a) exhibits the direct formation of one main photoproduct (peak at 4.25 min) accompanied by the generation of the dimeric azoxybenzene side product (peak at 4.5 min). In comparison, the elugram of CL-B (Figure 2b) displays the formation of an intermediary compound (peak at 6.6 min) during irradiation in addition to the main photoproduct (peak at 5.0 min). The intermediate was assigned to the compound generated by the unilateral cleavage of one *o*-nitrobenzylic ester group of the symmetric bifunctional molecule. Further irradiation leads to the complete cleavage of both chromophore units and therefore results in one main photoproduct, which was assigned to the peak at 5.0 min. It was demonstrated that the variation of the molecular structures of the cross-linkers CL-A and CL-B results in different degradation profiles whereas CL-A reacts around 1.5 times faster than CL-B. Taking into account absorption of the (intermediary) photoproducts in the same spectral region as the wavelengths used for the cleavage of the cross-linkers, the photoreaction of the two chromophores containing CL-B is significantly slowed down compared to CL-A. Nevertheless, even a unilateral cleavage of the CL-B molecule is assumed to already enable the degradation of a polymeric network. In addition, the complete cleavage of CL-B for longer irradiation times does not generate any polymer bound dimeric side products, which is expected to facilitate the complete particle degradation under mild conditions.

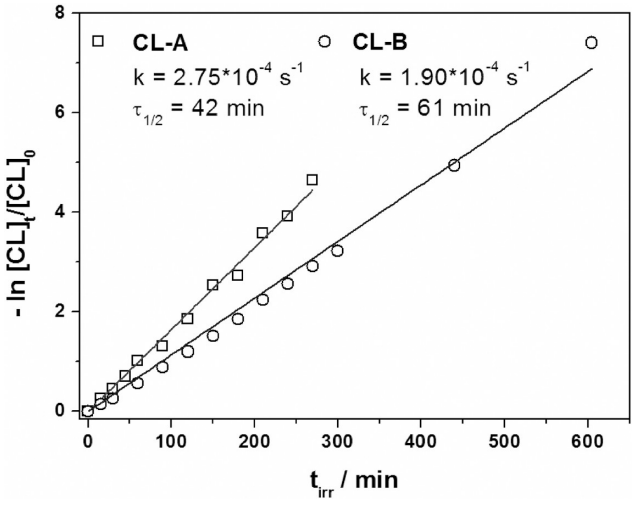

Figure 3. Kinetic investigations on the photolytic cross-linker degradation: Kinetic plots of $-\ln[CL]_t/[CL]_0$ versus irradiation time for CL-A and CL-B, respective rate constants and half times.

Preparation and Characterization of Cross-Linked Photo-Degradable p(HEMA-*co*-MAA) Hydrogel Nanoparticles by Inverse Miniemulsion Copolymerization. Regarding the preparation of polymeric nanoparticles by copolymerization of different monomers and cross-linkers, the miniemulsion polymerization technique is highly advantageous compared to other techniques for microgel preparation such as, e.g., precipitation polymerization. As the latter is strongly dependent on a specific hydrophobicity of the materials prepared, hydrophilic (co)monomers are only incorporable to a certain extent.[55] Moreover, it is limited to the utilization of water-soluble monomers.[20] In contrast, (inverse) miniemulsions are characterized by suppression of diffusion of compounds between droplets, rendering those as nanoreactors.[56−58] As a result the composition of the latex particles resembles the composition of the monomer phase in the droplets. In particular, for the copolymerization of different

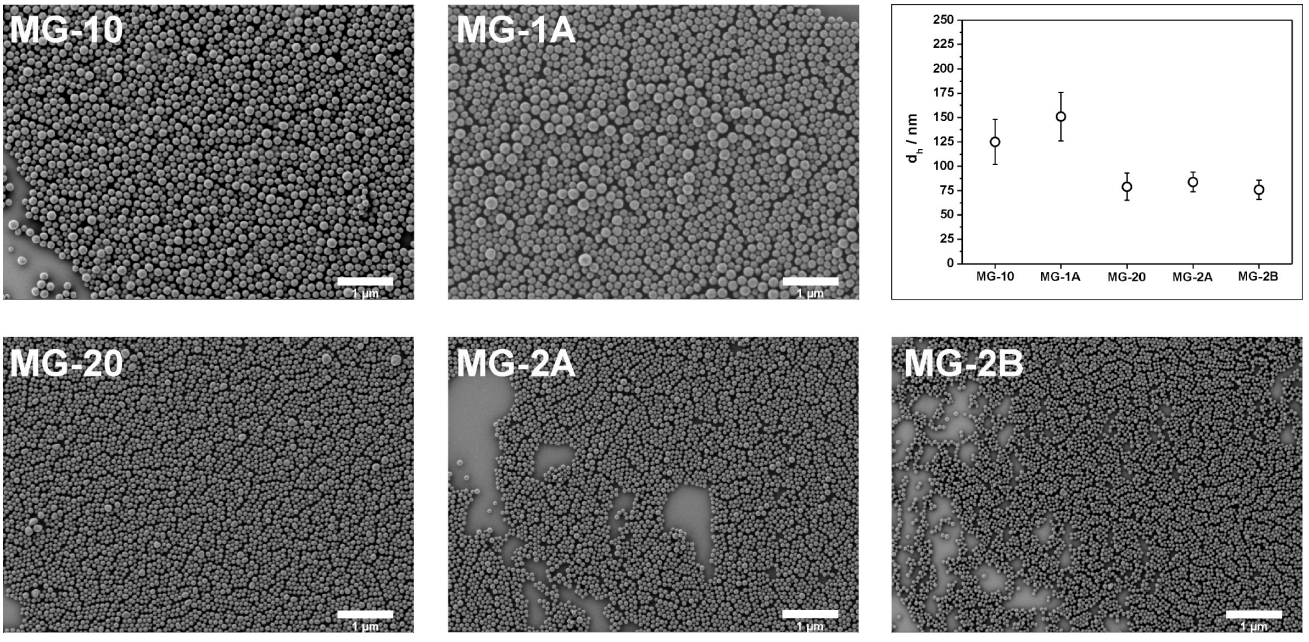

Figure 4. Representative SEM images of p(HEMA-*co*-MAA) microgels drop cast from cyclohexane dispersions and hydrodynamic diameters obtained from DLS measurements in cyclohexane.

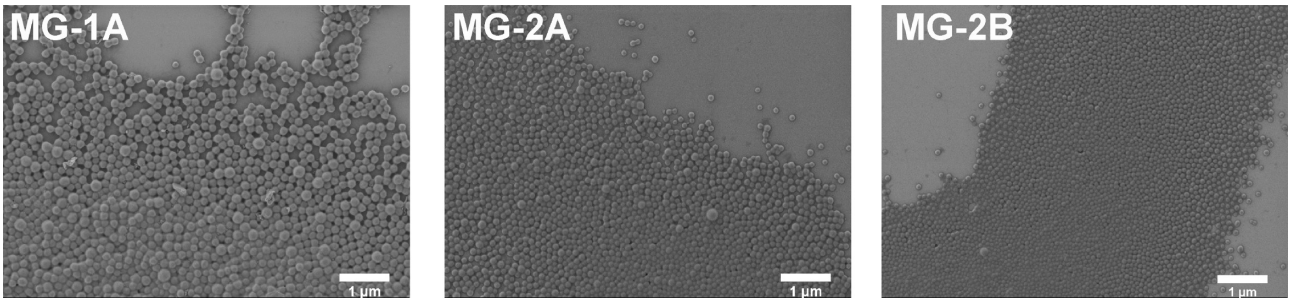

Figure 5. Representative SEM images of photodegradable p(HEMA-*co*-MAA) microgels drop cast from aqueous dispersions at pH 8.5.

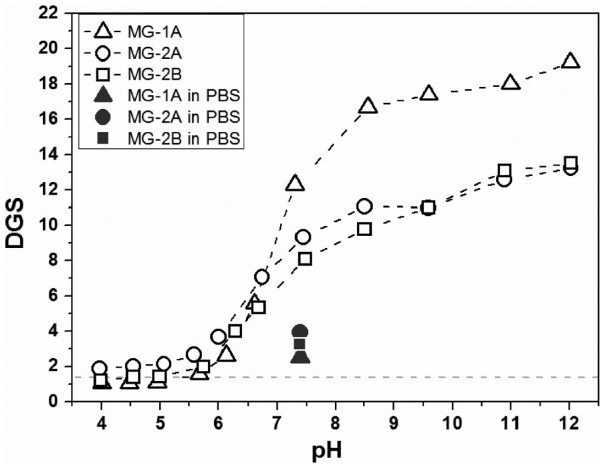

Figure 6. Investigations on the pH-dependent swelling behavior of photodegradable p(HEMA-*co*-MAA) microgels: degrees of swelling in dependency on pH and additional values for PBS as medium.

monomers and cross-linkers, this method allows the equal distribution of all functionalities incorporated. In addition, the preparation of microgels is not limited to water-soluble monomers since stable miniemulsions can also be obtained for dispersed phases consisting of organic solvents immiscible with the organic continuous phase.

Photodegradable p(HEMA-*co*-MAA) microgels were prepared by the copolymerization of HEMA, MAA, and the respective cross-linkers in inverse miniemulsion. In order to ensure comparability between the individual gel particles regarding their swelling and degradation behavior, 2.5 mol % of cross-linkers were used in every case. For the MG-1A microgels, the cross-linking molecule CL-A was readily soluble in the monomer mixture, so no further solvent was used to form the dispersed phase prior to polymerization. Solubility restrictions of CL-B in the same monomer composition hindered analogous reaction conditions. Therefore, in order to form MG-2B microgels, 20 w% of DMSO were added to ensure complete cross-linker solubility. Analogously, MG-2A gel particles were prepared using cross-linker CL-A. In addition, particles containing no cross-linking molecules were prepared as reference particles for the swelling and degradation experiments. P(HEMA-*co*-MAA) MG-10 nanoparticles were polymerized analogously to MG-1A gel particles without any additional solvent for the dispersed phase. In contrast, MG-20 particles, polymerized using 20 w% DMSO as solvent, represent the reference particles to the MG-2A and MG-2B microgels. To remove excess surfactant, all particle dispersions were repeatedly washed with cyclohexane after polymerization yielding stable dispersions. Hydrodynamic diameters of the nonswollen MGs were determined by DLS measurements in cyclohexane and were found to be in the size range of around 130 nm for MG-10 and MG-1A particles and about 85 nm for MG-20, MG-1A, and MG-2A microgels. For the miniemulsions including DMSO as solvent for the dispersed phase, smaller particles were obtained after polymerization. This effect might be either explained by a changed surface tension or a decreased viscosity in this system. Figure 4 shows representative SEM pictures of the drop cast cyclohexane dispersions on silica wafers together with the hydrodynamic diameters obtained from DLS measurements.

In order to transfer the prepared microgels to the aqueous phase, the freeze-dried samples were allowed to swell in water (solid content 5.0% (w/v)) adjusted to pH 12. Here, complete deprotonation of the carboxylic acid groups was achieved as could be monitored by the decrease of the pH to about pH 8 for all samples. After titration with diluted hydrochloric acid to pH 7, the swollen microgels were washed 3 times with deionized water to remove formed sodium chloride, unreacted monomers and non-cross-linked free polymer chains and oligomers. Freeze-drying of the purified dispersions yielded the microgels as slightly yellow colored powders which can be stored in the dried state and transferred to water by simple swelling. Resulting aqueous dispersions are stable without any additional surfactant due to sterical stabilization by dangling chains of the swollen outer layer of the microgels.

The retention of the particulate structure for the cross-linked particles dispersed in aqueous media of pH 8.5 was confirmed by SEM analysis. Figure 5 shows representative pictures. Because of the highly swollen state of the microgels prior to drying, the particles can be identified as flattened spheres on the wafer. No drastic morphological deviations from the samples dropcast from cyclohexane dispersion were observed. This is assumed to be the result of drying effects on the relatively hydrophobic silica surface: whereas in regions of high particle concentration interpenetration of the outer particle layers is visible, single or separated particles exhibit only slightly flattened morphologies of marginally increased diameters. non-cross-linked reference particles MG-10 and MG-20 completely dissolved in water and SEM analysis only showed polymer films but no spherical structures.

Investigations on the pH-Dependent Swelling Behavior of the Microgels. The prepared microgels are designed to exhibit a pH-dependent swelling behavior due to the anionic network-forming p(HEMA-*co*-MMA) copolymer. Deprotonation of the carboxylic acid groups increases the hydrophilicity of the network,

Table 2. Results from Titration Experiments on Photo-Degradable p(HEMA-*co*-MAA) Microgel Dispersions[a]

sample	Q / 10^{-3} mol/g	*IE* (MAA)/%	pK_a
MG-1A	1.26	81	6.30
MG-2A	1.17	77	6.28
MG-2B	1.16	75	6.27

[a] Obtained values for the content of ionizable groups Q, the incorporation efficiency IE of MAA and the pK_a values.

thus inducing an enlargement of the degree of swelling of the particles. This effect is even enhanced by electrostatic repulsion of the generated anionic groups at higher pH values.

With the aim to investigate the described behavior, the pH values of microgel dispersions in water were varied from pH 4 to pH 12 by adding an aqueous NaOH solution, and hydrodynamic diameters (d_h) of the particles were measured by DLS for every pH value. The resulting graphs of plotting d_h against pH are shown in Figure S2 in the Supporting Information. Figure 6 shows the resulting degrees of swelling calculated as DGS = $V_{swollen}/V_{nonswollen}$, where $V_{nonswollen}$ represents the values obtained for the particle dispersions in cyclohexane.

As expected, all microgels exhibited pH-dependent swelling properties with critical swelling transitions from the collapsed to the swollen state at pH values between 6.0 and 8.5. A detailed examination and discussion can be found in the Supporting Information. Comparing the actual relative volumes of the different particles, it is noteworthy that all microgels dispersed in phosphate buffer saline (PBS) with pH 7.4 showed a lower swelling degree compared to the identical particles in water of the same pH (see Figure 6). Cationic electrolytes present in the buffer solution shield the generated anionic groups in the network, thus resulting in a reduced electrostatic repulsion. Furthermore, it becomes obvious that the DGS values of MG-2A and MG-2B enlarged with increasing pH to a similar steady value of DGS_{max} = 11 at pH 8.5. In contrast, at the same pH, MG-1A is swollen to a much greater extend, as characterized by a higher maximum degree of swelling of DGS_{max} = 17. As MG-1A and MG-2A only differ in their preparation, namely their initial composition of the dispersed phase before the polymerization, it is assumed that this parameter either influences the amount of included cross-linker or the incorporation ratio of HEMA/MAA in the final network.

UV−vis measurements of microgel dispersions in DMSO were conducted to determine the amount of incorporated cross-linking molecules (see Supporting Information: Figure S3 and Figure S4). The relative quantity of incorporated cross-linker was determined with respect to HEMA and MAA amounts before polymerization as mol % of theory. Whereas in the case of MG-2A and MG-2B 73 and 82 mol % of CL-A and CL-B were incorporated into the respective microgels, for MG-1A a value of 117 mol % integration of CL-A was determined. Considering the pH-dependent swelling profile of the different microgels, an increased DGS_{max} of MG-1A in combination with a higher amount of incorporated cross-linker (>100 mol % of theory) is assumed to base on an enhanced incorporation of MAA into the network. Since the similar cross-linker incorporation efficiencies into the microgels, polymerized using additional DMSO as solvent (MG-2A and MG-2B), were found to vary significantly from the value for MG-1A, it is assumed that the composition of the dispersed phase during polymerization influences both

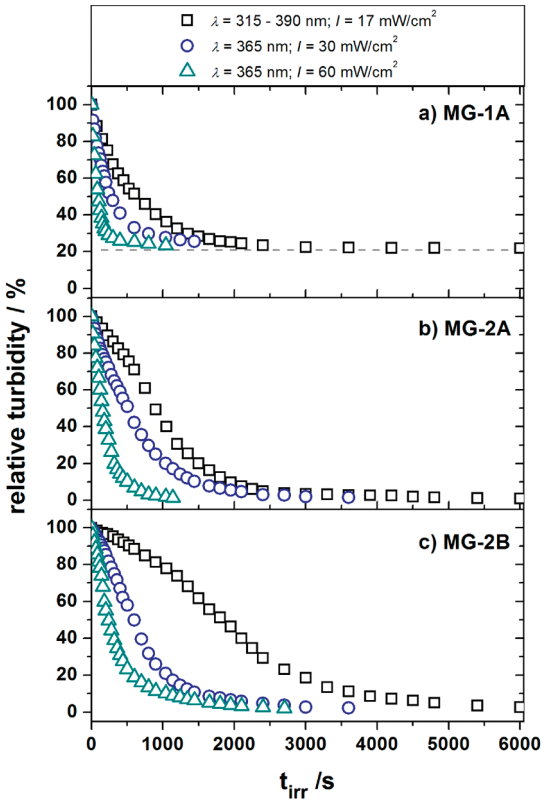

Figure 7. Investigations on the light-induced particle degradation at pH 8.5 by turbidity measurements for different light intensities and wavelengths for (a) MG-1A, (b) MG-2A, and (c) MG-2B.

parameters mentioned above: the cross-linker incorporation and the HEMA/MAA ratio in the network forming polymer. In general, nonquantitative conversions of the polymerization reactions yielded sol contents consisting of unreacted monomers, cross-linkers and non-cross-linked oligomer or polymer chains. Removal of the sol during gel purification therefore resulted in cross-linker incorporation efficiencies depending on the composition of the respective sol content and differing from the theoretical amount.

In order to investigate the proposed enhanced incorporation of MAA into MG-1A microgels, potentiometric titration experiments were conducted and yielded the contents of ionizable groups Q and the pK_a values of the microgels (see Supporting Information, Figure S5).[59] From the calculated values for Q, the MAA incorporation efficiency *IE* (MAA) was determined relative to the theoretical amount assuming 100% incorporation of monomers and cross-linkers into the latex particles. The obtained values are listed in Table 2.

It was demonstrated that for all samples the amount of integrated MAA groups in the microgels differs from the theoretical amount of 100%. Keeping in mind that the final composition of the polymeric gels is influenced by the conversion of the polymerization, this effect can be explained by removal of the sol content during the purification procedure which resulted in the observed deviations from the theoretical values. Nevertheless, MG-1A with $Q = 1.26 \times 10^{-3}$ mol/g clearly contains a higher percentage of acid groups than microgels MG-2A and MG-2B with $Q = 1.17 \times 10^{-3}$ mol/g and 1.16×10^{-3} mol/g, thus resulting in a higher degree of swelling despite an also enhanced

incorporation of cross-linking points. The observed pK_a values are in all cases in good agreement with the observed swelling profiles.

Photo-Degradation Experiments of p(HEMA-*co*-MAA) Microgels in Aqueous Media. Photodegradation of the different microgels in water was examined by irradiating 0.125% (w/v) dispersions in various aqueous media with UV light. The light-induced swelling/degradation was monitored by turbidity of the samples. Analogously to irradiation studies of photodegradable PMMA particles, turbidity was measured as the relative scattering intensity at 90°.[50] Here, the cleavage of cross-linking points leads to a looser network structure, thus decreasing the contrast in the refractive indices between solvent and particle.[60,61]

In a first attempt, dispersions of highly swollen microgels at pH 8.5 were irradiated with UV light of varying wavelengths and intensities. Figure 7 shows the resulting turbidity curves.

As can be seen in Figure 7a, irradiation of MG-1A microgels with UV light of the wavelengths of 315−390 nm and an intensity of 17 mW/cm^2 does only result in a decay of the turbidity down to a constant level of about 21%, therefore indicating only increased particle swelling due to incomplete degradation. In contrast, MG-2A and MG-2B both exhibit a decrease in scattering intensity to almost 0% of the initial value being a sign of complete particle disintegration. Furthermore, using a discrete irradiation wavelength of 365 nm and increasing the UV light intensity up to 30 and 60 mW/cm^2 results in a faster degradation for all microgels but does not influence the constant turbidity level >0% of MG-1A. In general, this behavior allows controlling the degradation rate via the light intensities used.

The differences of the degradation profiles of MG-1A and MG-2A microgels, both containing cross-linker CL-A, are based on their respective polymerization conditions. Whereas in the case of MG-1A no additional solvent was used during polymerization, MG-2A microgels were prepared by adding DMSO to the dispersed phase. As discussed above, this parameter influences the composition of the final gels in terms of amount of MAA groups in the network-forming copolymer and incorporated cross-linker molecules. As a higher cross-linker content was determined for MG-1A particles compared to MG-2A gels, the observed retardation of light induced particle disintegration can be explained. Nevertheless, increasing the irradiation light intensity does not affect the constant turbidity level observed for MG-1A latexes, therefore indicating the influence of another parameter. Irradiation of CL-A cross-linking molecules is known to form dimeric azoxybenzene side products. As shown for PMMA-gel particles, those side products are bound to the polymer backbone, therefore forming new cross-linking points hindering complete particle disintegration.[50] It is assumed that this effect also occurs in MG-1A microgels but is suppressed in the case of MG-2A. It is proposed that a higher degree of chain entanglement in combination with a higher amount of incorporated cross-linker in MG-1A microgels retards the diffusion of cleaved polymer chains in the gels, thus rendering the formation of dimers by the encounter of two polymer bound chromophores more likely. In this context, the use of additional DMSO as solvent for the dispersed phase of MG-2A is assumed to influence the resulting molecular weight of the gel forming polymers by restraining the Trommsdorff effect due to a higher dilution of the polymerization mixture. Even though reference particles MG-10 and MG-20 were completely soluble and disintegrated at pH 8.5, the determination of the molecular weights of the polymers by GPC analysis yielded values of M_n = 235 000 g/mol (PDI = 4.3)

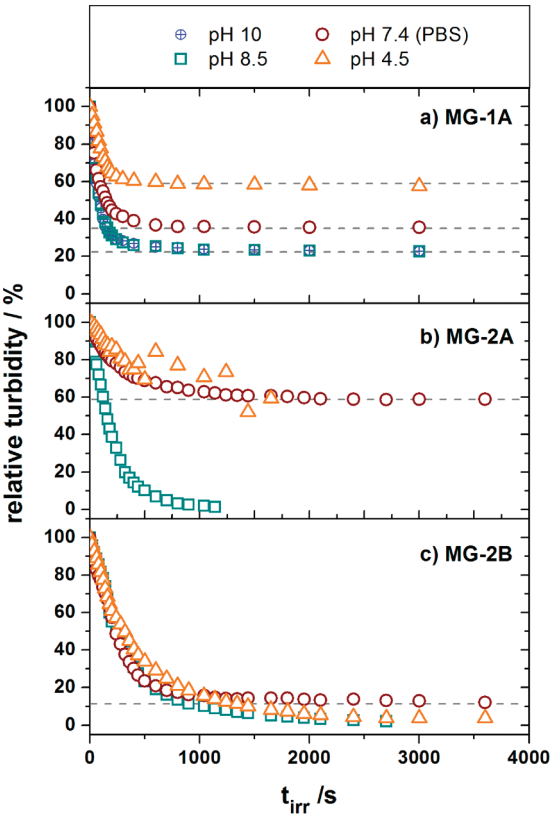

Figure 8. Investigations on the light-induced (λ = 365 nm; I = 60 mW/cm^2) particle degradation by turbidity measurements at different pH values for (a) MG-1A, (b) MG-2A, and (c) MG-2B.

and M_n = 53 000 g/mol (PDI = 2.0) for MG-10 and MG-20, respectively (see Figure S6 in the Supporting Information). The about five times increased molecular weight of the polymers formed without additional DSMO as well as the dramatically increased polydispersity point toward the occurrence of a gelation effect during the polymerization. It is concluded that incomplete particle degradation of MG-1A originates in the distinct photolysis behavior of CL-A in correlation with polymer entanglement of the network-forming copolymer.

Regarding possible release applications for the double stimuli-responsive microgels, a direct degradation of the collapsed particles at pH 4.5 would enable a one-step release, whereas the degradation of slightly swollen microgels in PBS would combine a primary slow diffusion-based release with a subsequent irradiation-based degradation, thus representing a two-step release profile. In order to examine the dependency of the light-triggered particle disintegration on the pH, irradiation experiments with UV light of λ = 365 nm and I = 60 mW/cm^2 were conducted in different aqueous media and reactions were monitored again by turbidity measurements. The obtained curves are shown in Figure 8.

The irradiation of MG-1A microgels in aqueous media at different pH resulted in every case in a decay of turbidity down to a constant level higher than 0%. Comparing the results obtained for pH 8.5 and 10, no differences in the turbidity curves were observed, thus confirming that incomplete particle degradation is a result of newly formed cross-links as side products of the photolysis of CL-A. Physical cross-links between the formed amine groups of cleaved CL-A and the carboxylic acid groups of

the network-forming copolymer can be excluded due to the absence of protonated amine moieties at this pH value. Measurements in PBS at pH 7.4 and aqueous medium at pH 4.5 resulted in an increase of the constant turbidity levels up to 32 and 60% respectively. Here, analogously to the experiments in basic media, irradiation of the microgels causes the cleavage of CL-A molecules and the formation of new cross-links as side reactions resulting in swollen gel particles rather than free polymer chains. The final degree of swelling after irradiation correlates to the constant turbidity level and is influenced by two parameters: (a) the ratio of CL-A cleavage to dimeric side product formation and (b) the pH-dependent swelling properties of the gels. An initial low degree of swelling due to a lower pH favors in this context the formation of new cross-links. A more confined space enhances the reaction probability of two polymer bound groups thus hindering particle swelling due to newly formed dimeric cross-links.

Experiments conducted on MG-2A microgels confirm the conclusions derived above. While complete degradation was observed for a high initial degree of swelling at pH 8.5, irradiations in PBS or pH 4.5 resulted in incomplete particle disintegration, characterized by final constant turbidity values of about 60%. At pH 8.5, in contrast to MG-1A latexes, reduced entanglement of the shorter polymer chains enables the generated photolysis products to diffuse apart sufficiently fast enough not to form dimeric side products. By lowering the pH and thereby reducing the initial degree of swelling, the spatial concentration of the photolysis products in the less swollen gels is increased, thus enabling the formation of new dimeric cross-links and resulting in swelling of the particles or formation of macroscopic aggregates rather than complete degradation.

Regarding MG-2B gel particles cross-linked with CL-B—independent of the pH of the media—the turbidity of the samples decreased upon irradiation in every case down to almost 0%, therefore indicating complete particle degradation. In contrast to MG-1A and MG-2A particles cross-linked with CL-A, CL-B—used to cross-link MG-2B—was designed to be cleaved upon irradiation without generating polymer bound chromophores. As a result, photolytic generation of dimeric side products prohibits the formation of new cross-links. The excellent and fast degradation behavior of MG-2B independent of the pH of the aqueous phase renders those particles highly interesting for possible release applications.

Investigations on the Double Stimuli-Responsive Behavior of the p(HEMA-*co*-MAA) Hydrogel Nanoparticles. Depending on the specific properties of the active compound to be delivered, the loading and release mechanisms due to an externally induced volume transition can vary significantly. While collapsing a microgel containing low molecular weight compounds electrostatically adsorbed to the former swollen network can induce its release,[20] a similar volume transition can be used to entrap high molecular weight compounds such as, e.g., proteins in the gel.[62] Here, the swollen state enables the diffusion of active compounds with a hydrodynamic diameter smaller than the mesh size of the swollen network in and out of the gel. Deswelling of the network is characterized by an effective decrease of the mesh size, therefore entrapping the active compound due to hindered diffusion. Subsequent swelling results then in the release of the captured compound.

Regarding the potential of the dual stimuli-sensitive photodegradable p(HEMA-*co*-MAA) microgels for release applications, pH-dependent swelling/deswelling of the gels should be combined

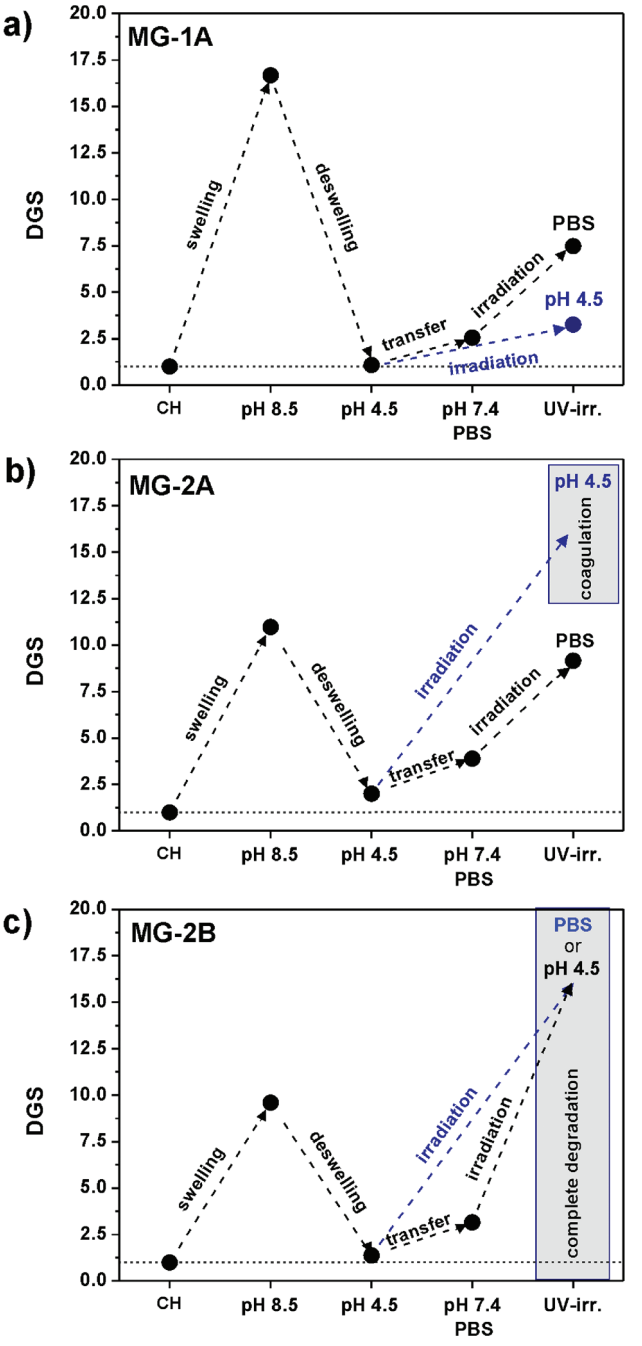

Figure 9. Investigations on the double stimuli-responsive behavior of photodegradable p(HEMA-*co*-MAA) microgels: pH-induced swelling and light-triggered (partial) degradation in different media. Plots of DGS in dependency on different stimuli and surrounding media for (a) MG-1A, (b) MG-2A, and (c) MG-2B.

with subsequent photodegradation. Figure 9 demonstrates the investigated responses in terms of the degree of swelling of the different microgel particles. It becomes obvious that all microgel particles can easily be transferred from the cyclohexane phase to aqueous media by swelling freeze-dried samples at pH values higher than pH 8. Lowering the pH to around 4.5 resulted in every case in deswelling of the microgels, therefore giving rise to a potential entrapment of active compounds in the network. Collapsed particles can then follow either a direct degradation or a

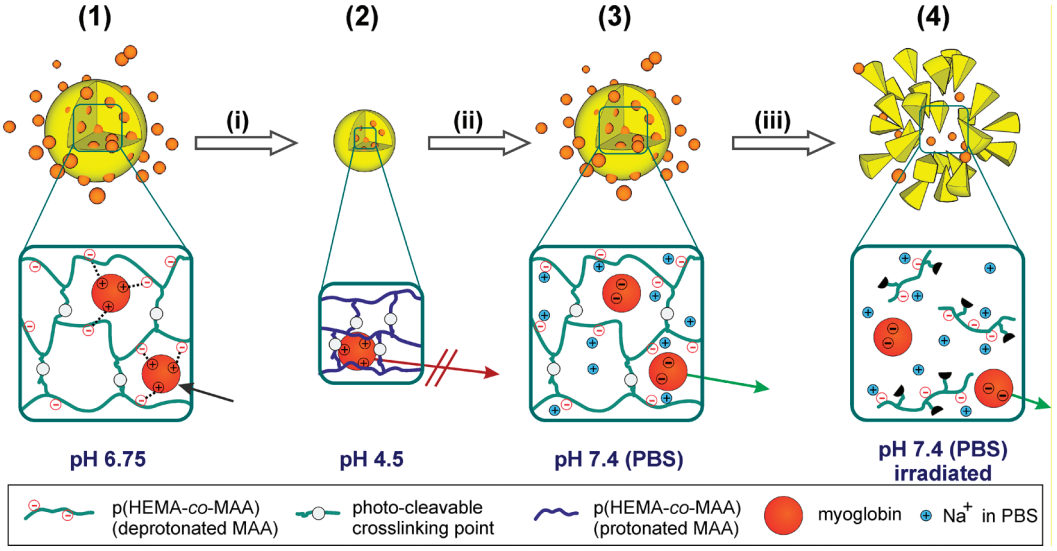

Figure 10. Schematic illustration of the loading and release strategy for p(HEMA-*co*-MAA) microgels. (1−2) Loading of large cationic functional compounds into the anionic gel: (i) entrapment by pH-induced deswelling. (3) Diffusion controlled release: (ii) reswelling in PBS. (4) Degradation controlled release: (iii) irradiation in PBS.

two-step swelling/degradation profile. Whereas the direct case represents the light-triggered degradation of the collapsed particles in acidic medium, the two-step profile can be realized by slightly swelling the particles in PBS which is then followed by (complete) particle degradation upon irradiation.

It was demonstrated that in the case of microgel particles MG-1A and MG-2A cross-linked with CL-A, the direct photolytic degradation of the collapsed particles in pH 4.5 is hindered by the formation of new cross-links and results only in slightly swollen particles or macroscopic coagulates. Nevertheless, swelling of these nonirradiated microgels in PBS is characterized by an initial small increase in the degree of swelling up to a DGS of about 3. Subsequent irradiation leads then to dramatic increases in the particle volumes to a DGS of about 8. This pronounced difference is assigned to increased mesh sizes, thus increasing the diffusion coefficients of potential embedded compounds in the swollen state. In contrast, due to the specific designed photolytic behavior of CL-B cross-linking molecules, MG-2B microgels can be fully degraded upon UV light irradiation either in acidic aqueous phase or in PBS.

Investigations on the Loading and Release of Myoglobin. Having demonstrated the successful combination of a well-defined pH-dependent swelling profile with the photolytic degradability of p(HEMA-*co*-MAA) microgels, their potential utilization for the loading and release of functional compounds is of high interest. A proposed loading and release mechanism of anionic p(HEMA-*co*-MAA) microgels is based on the following considerations which are schematically illustrated in Figure 10.

The gel particles are highly swollen in aqueous medium of pH values higher than pH 6.0 and consist of negatively charged networks of large pore sizes. Immersing the microgels in a solution of a substance with a hydrodynamic diameter smaller than the mesh sizes of the gel and positively charged at the respective pH, enables the diffusion of the functional compound into the network. Loading due to electrostatic interactions between the different ionic groups can therefore be achieved (see Figure 10(1)). In a next step the pH of the surrounding medium is lowered in order to induce a deswelling of the gel and thereby a decrease of the pore sizes of the network (Figure 10(i)). As a result, for substances of a hydrodynamic diameter larger than the pore sizes of the collapsed gel, their diffusion from the network is hindered even though the electrostatic interactions are also weakened. This approach is assumed to result in an entrapment of the respective compound (see Figure 10(2)). In this case, leakage of the payload from the collapsed microgels at low pH values is prevented.

Regarding the release of the embedded compounds, a two-step release profile based on the demonstrated two-step swelling and degradation profile (see Figure 10) is proposed. First, by increasing the pH to a value at which both the functional compound and the carboxylic acid groups in the network are negatively charged (Figure 10(ii)), the reduced electrostatic interactions between embedded substance and network in combination with the increased pore sizes of the swollen gel induce the release (see Figure 10(3)). Second, this first pH-dependent diffusion controlled release profile can be combined with either a subsequent or substitutional degradation-induced release upon irradiation (see Figure 10, parts iii and 4).

In order to examine the proposed method, investigations on the loading of MG-2B microgels with myoglobin and its subsequent release were carried out. Myoglobin was chosen as a model protein since it fulfills certain important criteria for the successful loading. The isoelectric point of myoglobin of $Ip = 7.0$ was shown to enable the successful loading into anionic microgels containing methacrylic acid groups at pH 6.75.[24] At this pH value it was demonstrated that the MG-2B microgels are highly swollen due to the presence of anionic charges in the network-forming copolymer. In addition, this particular pH value lower than the isolectric point of the protein renders the latter positively charged, thus enabling an efficient loading due to electrostatic interactions with the negatively charged gel. Moreover, the relatively large hydrodynamic diameter of around 4.4 nm of the globular protein (molecular weight of approximately 17 kDa) is assumed to facilitate the entrapment in the microgels upon deswelling. Another beneficial characteristic is

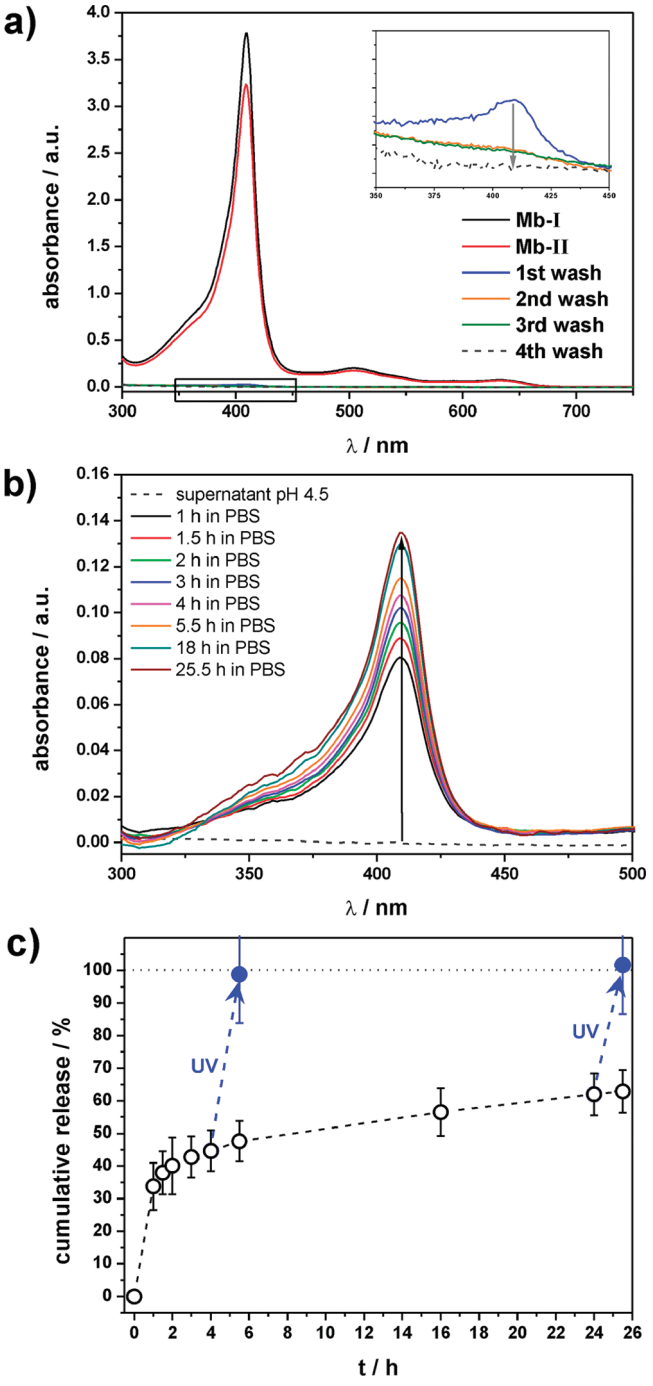

Figure 11. Investigations on the loading of myoglobin and its subsequent release from light-sensitive p(HEMA-*co*-MAA) microgels: (a) UV−vis spectroscopic examination of the loading process of MG-2B microgels with myoglobin; (b) time-dependent UV−vis spectra of the release of myoglobin from MG-2B microgels in PBS at 37 °C; (c) cumulative release dependency on the incubation and irradiation time. The dotted line is a guide to the eyes.

the UV absorption maximum at λ_{max} = 410 nm, which permits both the determination of loading efficiencies and the monitoring of the release by UV−vis spectroscopy. Furthermore, the comparably low absorption of the protein in the spectral region used for the irradiation is beneficial (see Figure S7 in the Supporting Information).

Following a procedure described by Eichenbaum et al.,[25] loading of anionic p(HEMA-*co*-MAA) MG-2B microgels with myoglobin was performed by immersing the gel particles overnight in a solution of the protein at pH 6.75. After equilibration, the pH of the dispersion was adjusted to pH 4.5 in order to collapse the microgels and entrap the embedded protein. Afterward, the microgel particles were separated by centrifugation, the supernatant was removed and the particles were redispersed in water with pH 4.5. After repeatedly washing the loaded particles, the microgels were finally redispersed in PBS. The loading process was monitored by UV−vis spectroscopy (see Figure 11a). Comparing the UV−vis spectrum of a myoglobin reference solution (Mb-I) (of the same concentration as used for the loading experiments) at pH 4.5 to the spectrum of the supernatant (Mb-II) (after removal of the loaded and collapsed microgels by centrifugation), it can be seen that the intensity of the absorbance at λ_{max} = 410 nm decreased significantly. The observed difference can be attributed to a removed amount of myoglobin from the solution therefore indicating successful loading of the protein into the microgels by entrapment. The subsequent washing steps were conducted to remove excess myoglobin. By adjusting the pH value of the surrounding medium to pH 4.5, carboxylic acid groups are protonated and the electrostatic interaction with the positively charged myoglobin is weakened. While protein molecules in the microgel interior are entrapped due to the decreased pore sizes of the gel network, loosely adsorbed myoglobin molecules on the surface of the particles are assumed to be liberated. Therefore, multiple washing steps with water of pH 4.5 were conducted to remove physically adsorbed proteins. The UV−vis spectra of the supernatants of the performed washing steps did not show a significant absorbance in the wavelength region of λ_{max} of myoglobin after the second washing cycle. Hence, the absence of myoglobin in the washing phases points toward an efficient entrapment accompanied by the successful suppression of leakage at the respective low pH value of 4.5. After the last centrifugation step, the microgels were redispersed in PBS.

Calculation of loading- (LE) and embedding efficiency (EE) (see Supporting Information) afforded the values of LE = 53.2 ± 7.4% and EE = 6.3 ± 0.9%. Regarding the high loading efficiency of 53.2% it can be concluded that the investigated approach of loading myoglobin upon entrapment of the protein in collapsed MG-2B microgels is a very efficient process. The relatively low embedding efficiency of 6.9% can be assigned to a huge excess of myoglobin with respect to the amount of microgels. Nevertheless, the examined loading strategy allows the recycling of not incorporated myoglobin since the microgels were easily removed from the solution by centrifugation.

Having demonstrated the efficient loading of myoglobin in MG-2B microgels, in a next step the subsequent diffusion controlled release of the protein was investigated by transferring the loaded microgels from water of pH 4.5 to PBS of pH 7.4. The resulting microgel dispersion was shaken at 37 °C and samples were taken after predetermined time intervals. After removal of the microgels by centrifugation of each sample, the released amount of myoglobin in the supernatant was determined by comparing the UV absorbance at λ_{max} = 410 nm to a calibration curve of myoglobin in PBS (see Supporting Information, Figure S8). Here, performed control experiments ensured that centrifugation did not result in sedimentation of the pure protein (see Supporting Information, Figure S9).

In order to investigate the photodegradation-induced release of the protein, after 4 and 24 h of incubation, samples were taken and irradiated (1.5 h, λ = 315−390 nm). To ensure complete particle disintegration, irradiations were carried out until the relative turbidity of the samples dropped below 5% of their initial values. The release of the protein was then calculated from the absorption spectra of the resulting clear solutions. Here, it is noteworthy that the UV absorbance of the photoproducts of the cleavable cross-linker CL-B can have a potential influence on the spectroscopic quantification of the amount of free protein. Therefore, the respective spectra were calculated by subtracting a baseline of irradiated "empty" microgels in PBS (of the same concentration). Furthermore, it is known that irradiation of oxymyoglobin (MbO_2) leads to photodissociation to (Mb) and photo-oxidation to metmyoglobin (MMb).[63−65] Since these compounds exhibit different absorption spectra, irradiation-induced changes in the absorbance of the protein have to be considered in order to enable an accurate quantification of the released protein. For this, a control sample of pure myoglobin (of the same concentration as in the loaded microgel dispersion) in PBS was irradiated and the change in absorbance at 410 nm was calculated relative to the nonirradiated sample. The amount of released myoglobin was then obtained by taking this parameter into account. Figure 11b shows the measured time-dependent UV−vis spectra of the diffusion controlled release experiment in PBS and Figure 11c depicts the cumulative release of the protein in dependency on the incubation and irradiation time.

The increasing absorbance at λ_{max} = 410 nm in the time-dependent UV−vis spectra clearly demonstrates an increase of the concentration of myoglobin in the supernatants after centrifugation. By transferring the loaded, collapsed particles from pH 4.5 to PBS of pH 7.4, the loaded myoglobin is assumed to be released due to a combination of different factors. First, the particles exhibit an increased degree of swelling in the medium of increased pH, therefore consisting of larger pore sizes which enable a diffusion of the protein from the network. Second, even though the carboxylic acid groups in the network forming copolymer are assumed to be protonated at pH 7.4, this pH value is higher than the isoelectric point of myoglobin (Ip = 7.0). Thus, the protein is also mainly negatively charged. The resulting electrostatic repulsion between the anionic groups in the network and on the protein results in the release from the gel. Third, the high ionic strength of the buffer solution induces a shielding of anionic groups in the network. Moreover, the sodium counterions are assumed to displace electrostatic interactions between remaining positive charges of the protein and anionic carboxylate groups of the gel network therefore minimizing attractive physical interactions.

On the basis of the UV−vis spectroscopic investigations, the cumulative release was calculated. The observed diffusion controlled release profile (see Figure 11c) was found to follow an initial burst release of around 40% of myoglobin during the first 3 h of incubation in combination with a slow additional release of about 20% of embedded protein over a 22.5 h time span. Since the maximum release after 25.5 h of incubation was determined to be 62% of the loaded amount, it can be stated that a quantitative release was not achieved by the purely diffusion controlled mechanism in this time span. It is assumed that this retardation behavior is based on the equilibration between the release of myoglobin and the repenetration/diffusion of myoglobin into the highly swollen networks. Since the surrounding medium was not changed, it is proposed that the release profile depends on the concentration of myoglobin in the local environment of the microgels.

Regarding the light-induced release of myoglobin by photodegradation of the microgel networks, it can be seen from the graph in Figure 11c that this method enables a quantitative release at any desired time point. In comparison to the diffusion controlled profile, it was shown that the amount of released protein can hereby be increased by around 65% at 5.5 h and by 40% at 25.5 h of incubation thus enabling a very efficient light-induced release. In summary, it can be stated that a novel two-step release profile was realized by combining the pH-dependent swelling and the light-induced degradation of these materials.

CONCLUSION

Novel photodegradable p(HEMA-*co*-MAA) microgels were prepared by free radical inverse miniemulsion copolymerization of HEMA and MAA with two newly synthesized photolabile cross-linking molecules. The pH-dependent swelling behavior induced by the protonation/deprotonation of the methacrylic acid groups in the network-forming polymer, was found to exhibit large differences of the particle volumes in acidic and basic media. UV light irradiation led to particle disintegration caused by cleavage of the photolabile cross-linking points. The particular combination of the stimuli described is designed as a new strategy to two different swelling/degradation profiles. By exploiting these mechanisms, p(HEMA-*co*-MAA) MG-2B microgels were successfully loaded with myoglobin as a model protein by electrostatic interactions of the positively charged myoglobin molecules with the negatively charged polymeric gel in combination with large pore sizes of the swollen network. Subsequent entrapment of the compound by pH-induced deswelling of the particles resulted in a high loading efficiency, thus rendering this newly developed approach highly effective. The observed diffusion controlled release profile upon swelling the particles under physiological conditions followed an initial burst release in combination with a slow release over a prolonged period of time.

In addition, it was demonstrated that a subsequent fast and quantitative on-demand release could be realized by the application of UV light thereby representing a novel two-step release profile.

While the observed purely diffusion controlled release profile is very promising for a fast provision of a medium concentration of the compound in combination with a subsequent steady supply for a longer period of time, especially the additional ability to induce a fast and quantitative on-demand release upon the application of UV light in a noncontact approach, renders this new concept very interesting for delivery applications, e.g., in materials science or biomedical fields.

ASSOCIATED CONTENT

Supporting Information. UV−vis investigations on the photolysis of cleavable cross-linkers in solution, pH-dependent DLS measurements and titration curves of microgels, UV−vis spectroscopic determination of cross-linker incorporation, GPC measurements, and UV−vis spectroscopic investigations for the loading and release experiments. This material is available free of charge via the Internet at http://pubs.acs.org/.

AUTHOR INFORMATION

Corresponding Author
*E-mail: landfester@mpip-mainz.mpg.de.

ACKNOWLEDGMENT

D.K. acknowledges the International Max Planck Research School (IMPRS) for financial support. We thank Sebastian Goerres for conducting titration experiments.

REFERENCES

(1) Zha, L.; Banik, B.; Alexis, F. *Soft Matter* **2011**, *7* (13), 5908–5916.
(2) Karg, M.; Pastoriza-Santos, I.; Perez-Juste, J.; Hellweg, T.; Liz-Marzan, L. M. *Small* **2007**, *3*, 1222–1229.
(3) Sorrell, C. D.; Carter, M. C. D.; Serpe, M. J. *Adv. Funct. Mater.* **2011**, *21* (3), 425–433.
(4) Debord, J. D.; Lyon, L. A. *J. Phys. Chem. B* **2000**, *104* (27), 6327–6331.
(5) Kawaguchi, H.; Fujimoto, K. *Bioseparation* **1998**, *7* (4−5), 253–258.
(6) Welsch, N.; Ballauff, M.; Lu, Y., In *Chemical Design of Responsive Microgels*; Pich, A. R. W., Ed.; Springer: Berlin, 2010; Vol. 234, pp 129−163.
(7) Ballauff, M.; Lu, Y. *Polymer* **2007**, *48* (7), 1815–1823.
(8) Lu, Y.; Mei, Y.; Drechsler, M.; Ballauff, M. *Angew. Chem., Int. Ed.* **2006**, *45* (5), 813–816.
(9) Hamidi, M.; Azadi, A.; Rafiei, P. *Adv. Drug Delivery Rev.* **2008**, *60* (15), 1638–1649.
(10) Vinogradov, S. V. *Curr. Pharm. Des.* **2006**, *12* (36), 4703–4712.
(11) Pich, A.; Richtering, W. In *Chemical Design of Responsive Microgels*; Pich, A., Richtering, W., Eds.; Springer: Berlin, 2010; Vol. 234, pp 1−37.
(12) Malmsten, M.; Bysell, H.; Hansson, P. *Curr. Opin. Colloid Interface Sci.* **2010**, *15* (6), 435–444.
(13) Peppas, N. A.; Huang, Y.; Torres-Lugo, M.; Ward, J. H.; Zhang, J. *Annu. Rev. Biomed. Eng.* **2000**, *2*, 9–29.
(14) Das, M.; Zhang, H.; Kumacheva, E. *Annu. Rev. Mater. Res.* **2006**, *36*, 117–142.
(15) Lin, C.-C.; Metters, A. T. *Adv. Drug Delivery Rev.* **2006**, *58* (12−13), 1379–1408.
(16) Nayak, S.; Lee, H.; Chmielewski, J.; Lyon, L. A. *J. Am. Chem. Soc.* **2004**, *126* (33), 10258–10259.
(17) Nayak, S.; Lyon, L. A. *Angew. Chem., Int. Ed.* **2005**, *44* (47), 7686–7708.
(18) Wells, L. A.; Sheardown, H. *Eur. J. Pharm. Biopharm.* **2007**, *65* (3), 329–335.
(19) Dou, H.; Jiang, M. *Polym. Int.* **2007**, *56* (10), 1206–1212.
(20) Das, M.; Mardyani, S.; Chan, W. C. W.; Kumacheva, E. *Adv. Mater.* **2006**, *18* (1), 80–83.
(21) Qiu, Y.; Park, K. *Adv. Drug Delivery Rev.* **2001**, *53* (3), 321–339.
(22) Lin, C. C.; Metters, A. T. *Adv. Drug Delivery Rev.* **2006**, *58* (12−13), 1379–1408.
(23) Murthy, N.; Thng, Y. X.; Schuck, S.; Xu, M. C.; Frechet, J. M. J. *J. Am. Chem. Soc.* **2002**, *124* (42), 12398–12399.
(24) Eichenbaum, G. M.; Kiser, P. F.; Dobrynin, A. V.; Simon, S. A.; Needham, D. *Macromolecules* **1999**, *32* (15), 4867–4878.
(25) Eichenbaum, G. M.; Kiser, P. F.; Shah, D.; Simon, S. A.; Needham, D. *Macromolecules* **1999**, *32* (26), 8996–9006.
(26) Sankaranarayanan, J.; Mahmoud, E. A.; Kim, G.; Morachis, J. M.; Almutairi, A. *ACS Nano* **2010**, *4* (10), 5930–5936.
(27) Franssen, O.; Stenekes, R. J. H.; Hennink, W. E. *J. Controlled Release* **1999**, *59* (2), 219–228.
(28) De Geest, B. G.; De Koker, S.; Demeester, J.; De Smedt, S. C.; Hennink, W. E. *Polym. Chem.* **2010**, *1* (2), 137–148.
(29) Chong, S.-F.; Chandrawati, R.; Staedler, B.; Park, J.; Cho, J.; Wang, Y.; Jia, Z.; Bulmus, V.; Davis, T. P.; Zelikin, A. N.; Caruso, F. *Small* **2009**, *5* (22), 2601–2610.
(30) Jhaveri, S. B.; Carter, K. R. *Macromolecules* **2007**, *40*, 7874–7877.
(31) Goh, S. L.; Murthy, N.; Xu, M. C.; Frechet, J. M. J. *Bioconjugate Chem.* **2004**, *15* (3), 467–474.
(32) Bulmus, V.; Chan, Y.; Nguyen, Q.; Tran, H. L. *Macromol. Biosci.* **2007**, *7* (4), 446–455.
(33) Murthy, N.; Xu, M. C.; Schuck, S.; Kunisawa, J.; Shastri, N.; Frechet, J. M. J. *Proc. Natl. Acad. Sci. U.S.A.* **2003**, *100* (9), 4995–5000.
(34) Standley, S. M.; Kwon, Y. J.; Murthy, N.; Kunisawa, J.; Shastri, N.; Guillaudeu, S. J.; Lau, L.; Frechet, J. M. J. *Bioconjugate Chem.* **2004**, *15* (6), 1281–1288.
(35) Reichmanis, E.; Smith, B. C.; Gooden, R. *J. Polym. Sci., Part A: Polym. Chem.* **1985**, *23* (1), 1–8.
(36) Holmes, C. P. *J. Org. Chem.* **1997**, *62* (8), 2370–2380.
(37) del Campo, A.; Boos, D.; Spiess, H. W.; Jonas, U. *Angew. Chem., Int. Ed.* **2005**, *44* (30), 4707–4712.
(38) Wong, W. K.; Schupp, H.; Schnabel, W. *Macromolecules* **1989**, *22* (5), 2176–2181.
(39) Barzynski, H.; Sanger, D. *Angew. Makromol. Chem.* **1981**, *93* (FEB), 131–141.
(40) Katz, J. S.; Doh, J.; Irvine, D. J. *Langmuir* **2006**, *22* (1), 353–359.
(41) Piggott, A. M.; Karuso, P. *Tetrahedron Lett.* **2005**, *46* (47), 8241–8244.
(42) Kloxin, A. M.; Kasko, A. M.; Salinas, C. N.; Anseth, K. S. *Science* **2009**, *324* (5923), 59–63.
(43) Dvir, T.; Banghart, M. R.; Timko, B. P.; Langer, R.; Kohane, D. S. *Nano Lett.* **2010**, *10* (1), 250–254.
(44) Babin, J.; Pelletier, M.; Lepage, M.; Allard, J. F.; Morris, D.; Zhao, Y. *Angew. Chem., Int. Ed.* **2009**, *48* (18), 3329–3332.
(45) Jiang, J. Q.; Tong, X.; Morris, D.; Zhao, Y. *Macromolecules* **2006**, *39* (13), 4633–4640.
(46) Jiang, J. Q.; Tong, X.; Zhao, Y. *J. Am. Chem. Soc.* **2005**, *127* (23), 8290–8291.
(47) Zhao, Y. *Chem. Rec.* **2007**, *7*, 286–294.
(48) Li, Y.; Xinru, J.; Min, G.; Kuang, G.; Wei, Y. *J. Polym. Sci., Part A: Polym. Chem.* **2010**, *48*, 551–557.
(49) Burakowska, E.; Zimmerman, S. C.; Haag, R. *Small* **2009**, *5* (19), 2199–2204.
(50) Klinger, D.; Landfester, K. *Soft Matter* **2011**, *7* (4), 1426–1440.
(51) Holmes, C. P.; Jones, D. G. *J. Org. Chem.* **1995**, *60* (8), 2318–2319.
(52) Buhler, S.; Lagoja, I.; Giegrich, H.; Stengele, K. P.; Pfleiderer, W. *Helv. Chim. Acta* **2004**, *87* (3), 620–659.
(53) Braun, D.; Berger, J. *Kolloid Z. Z. Polym.* **1972**, *250* (2), 142–147.
(54) Conforti, P. F.; Garrison, B. J. *Chem. Phys. Lett.* **2005**, *406* (4−6), 294–299.
(55) Nayak, S.; Lyon, L. A. *Angew. Chem., Int. Ed.* **2005**, *44* (47), 7686–7708.
(56) Landfester, K.; Musyanovych, A. In *Chemical Design of Responsive Microgels*; Pich, A., Richtering, W., Eds.; Springer: Berlin, 2010; Vol. 234, pp 39−63.
(57) Landfester, K. *Angew. Chem., Int. Ed.* **2009**, *48* (25), 4488–4507.
(58) Landfester, K.; Willert, M.; Antonietti, M. *Macromolecules* **2000**, *33* (7), 2370–2376.
(59) Kawaguchi, S.; Yekta, A.; Winnik, M. A. *J. Colloid Interface Sci.* **1995**, *176* (2), 362–369.
(60) Al-Manasir, N.; Zhu, K. Z.; Kjoniksen, A. L.; Knudsen, K. D.; Karlsson, G.; Nystrom, B. *J. Phys. Chem. B* **2009**, *113* (32), 11115–11123.
(61) Lecner, M. D. *J. Serb. Chem. Soc.* **2005**, *70* (3), 361–369.
(62) Zhang, Y.; Zhu, W.; Wang, B. B.; Ding, J. D. *J. Controlled Release* **2005**, *105* (3), 260–268.
(63) Ma, J. Y.; Zheng, X. F.; Tang, Q.; Ma, J.; Gao, D.; H., H. J. *Sci. China, Ser. B* **2008**, *51* (5), 414–419.
(64) Hutchinson, J. A.; Noe, L. J. *J. Quantum Electron.* **1984**, *20* (12), 1353–1362.
(65) Bertelsen, G.; Skibsted, L. H. *Meat Sci.* **1987**, *19*, 243–251.